

# Evaluation methods for integrated normal multipoles in 3D magnet models

Nicolas Ruiz  
Direction: Jay Benesch

## **Abstract**

The numerical method used so far at Jefferson Lab to evaluate the multipole components in Opera 3D TOSCA magnet models, inspired on the experimental method using rotating coils is described in the first part of this document.

As its results are not flawless when it comes to evaluating normal quadrupole, it is challenged in a second chapter by a new evaluation method, inspired from the mathematical definition of the quadrupole term of the field expansion. After some adjustments this new method appears to give results that differ significantly from the former one.

In the third chapter the two methods are reconciled by the introduction of an analytical term standing for the geometrical effects that were not taken into account in the first method. As the corrected initial method and the new one eventually agree within a few percents prior to any optimization in the reconciliation process and to the percent level in the end, a greater confidence is gained in those numerical methods regarding their physical relevance as our understanding of the physical processes at stake gets finer.

# Table of contents

<b>I - Field multipoles evaluation method with circles</b> .....	3
I.1 - Presentation.....	3
I.2 - Limits of the method.....	4
<b>II - Field multipoles evaluation method with trajectory integrals</b> .....	6
II.1 - Presentation.....	6
II.2 - Results.....	8
II.2.1 - Field evaluation by nodal interpolation.....	8
II.2.2 - Field evaluation by surface integrals .....	11
<b>III - Reconciliation</b> .....	14
III.1 - Presentation.....	14
III.2 - Results.....	14
<b>IV - Conclusions and suggestions</b> .....	17
IV.1 - Conclusions.....	17
IV.2 - Suggestions.....	17
<i>Acknowledgements</i> .....	18
<i>References</i> .....	18

## I - Field multipoles evaluation method with circles

### I.1 - Presentation

Until now, it is the method that has always been used at Jefferson Lab to evaluate field multipoles in TOSCA models. The numerical code used in this study [1] to model the dipoles and compute their field has features that allow to measure the quality of the field induced by modeled magnets in a way that is very similar to the rotating coil technique, so that it is possible to compare the results of calculations with measured data when available.

In the real measurements that are made at Jlab, the coil rotates around the expected beam path and is then moved longitudinally to measure the field along the beam trajectory. As the quantity measured is the amount of flux cut by the coil, all the harmonics are summed and cannot be measured independently. More advanced devices are able to separate the harmonics via a set of multiple dedicated coils.

In the simulated models, the field is evaluated along a circle in a plane normal to the beam trajectory (Fig. 1&2). The circle is then displaced along a trajectory that follows the expected beam path - e.g. a circular path within a bending dipole field - and the field is evaluated at each step. A Fourier fit is computed from the circular field evaluation along each circle, simulating the values that would be measured for the field multipoles using rotating coils in a real magnet.

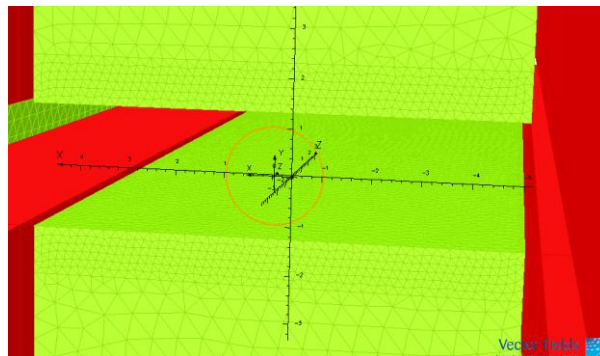


Fig. 1: Representation of the 1-cm circle around which the fields are evaluated in the simulated models. Green is the steel (magnet poles on this picture). The coils are in red.

The circles used to evaluate the 'ABH' magnet models have a radius of 1 cm. This value has been decided upon according to several criteria:

- 1) The radius cannot be much larger for the magnet poles are only 1.295 cm away from the beam trajectory (and thus from the center of the circle) and a circle evaluating fields too close to the poles would see its evaluation accuracy reduced due to irregularities in the mesh inherent to a change of medium.

2) Since the fields around the circle are evaluated by nodal interpolation, the perimeter of the circle has to be sufficient for the number of finite elements available for the interpolation along the circle to satisfy the sampling theorem.

3) One can use the fact that each  $2n$ -pole term in the field decomposition is proportional to  $r^{n-1}$  so that even evaluations made with a large circle can eventually lead to an evaluation at a beam-radius scale.

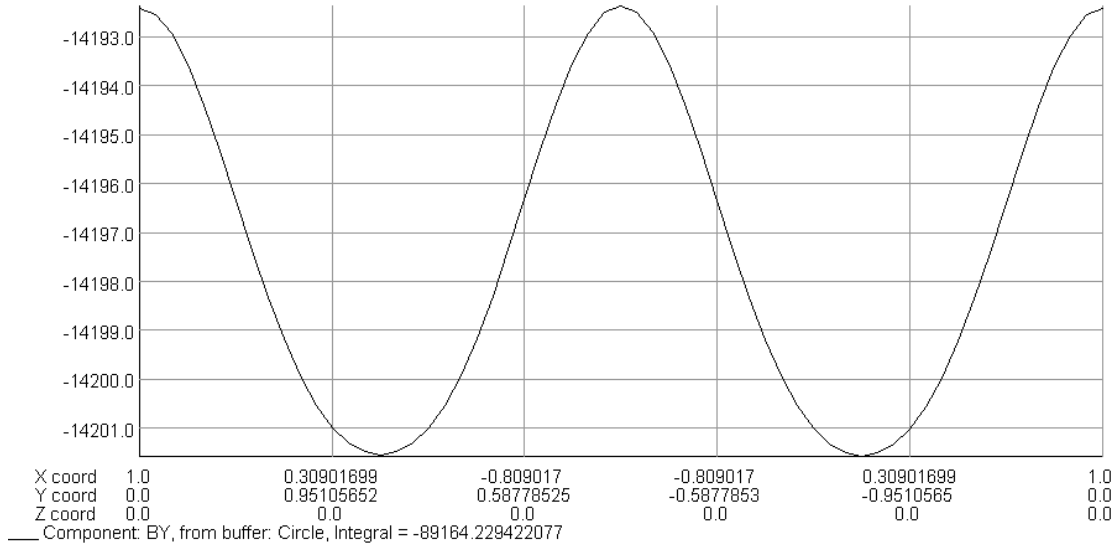


Fig. 2: Field evaluation around a 1-cm radius circle situated in the center of an 'ABH' dipole model.



## I.2 - Limits of the method

Although this method has been giving satisfying results for local scale study of the property of the magnetic field, it turns out that it suffers a major flaw when it comes to the evaluation of integrated normal quadrupole along the beam path. Normal quadrupole can be interpreted as the local variation of the normal dipole term. Since each circle is used to evaluate this variation locally, the integration along the beam path is therefore computed as follows:

$$\int \frac{\partial}{\partial x, y} B_y dl \quad (1)$$

That's to say the integration is calculated after the local variation of the dipole term is evaluated. This method's flaw comes from the fact that the circles are created normal to the trajectory of the beam, for local accuracy purposes. Since the circles have a radius of 1 cm (minimum size allowed by mesh density) and the beam trajectory is mainly circular in the dipole field, it turns out that the integration path length is affected by the size of the circles and trajectories that should have the same length (Fig. 3) are distorted, thus introducing a bias in the evaluation of geometrical effects.

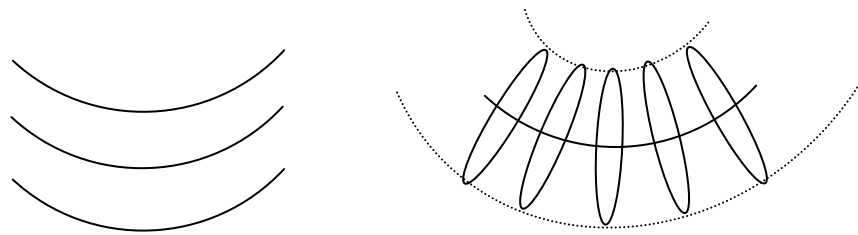


Fig. 3: Schematic representation of electron trajectories in a dipole field. Scheme on the left represents realistic trajectories of particles entering an homogenous dipole field, with different initial position but with equal radii of curvature. Scheme on the right shows the assumed trajectories that the method using circles implies, showing the distorted length and radii of curvature of the trajectories represented with dotted lines.

As a result the natural compensation that should exist between the difference in path length that causes weak focusing on the one hand and the edge effects caused by the non-normal incidence on the other hand doesn't appear on the results and the integrated field value obtained is unusable.

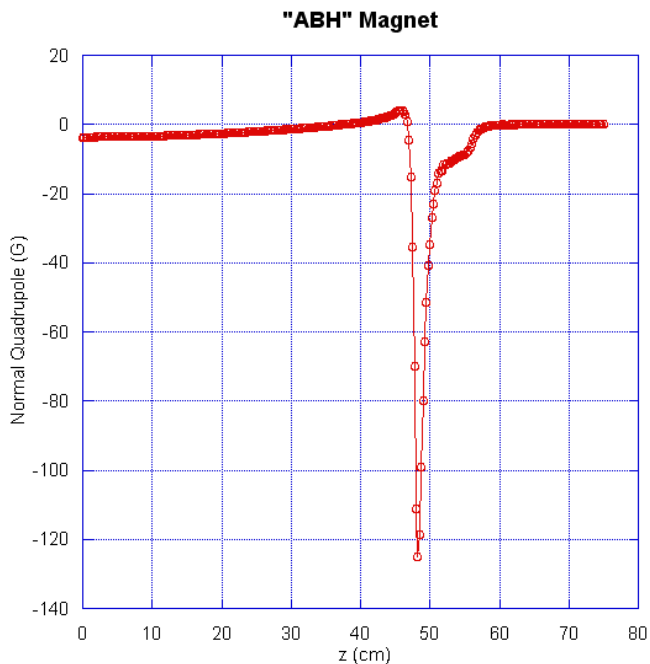


Fig. 4: Normal quadrupole field along the length of the "ABH" magnet. Note peak area is not compensated by the body value. '0' is the center of the magnet. Steel ends at z=48cm.

It was therefore decided that a new method ought to be developed to be able to evaluate correctly the integrated normal quadrupole content of those dipole magnet models.

## II - Field multipoles evaluation method with trajectory integrals

### II.1 - Presentation

The purpose of this method is to focus the evaluation on the integral and to deduce the quadrupole term from it instead of calculating the quadrupole locally and compute the integral out of it. The idea is to calculate :

$$\frac{\partial}{\partial x, y} \int B_y dl \quad (2)$$

Instead of:

$$\int \frac{\partial}{\partial x, y} B_y dl \quad (3)$$

Equations (2) and (3) are not equivalent in a non-Euclidian reference frame like the one implied by the curved path of the beam. Concretely, the normal dipole term of the field is directly evaluated and summed along the trajectory of the particle by the post processor of the numerical code. This operation is repeated for different values of the initial position of the particle and the normal quadrupole term is computed from the variation of the integral of the dipole term as the initial position varies along x or y.

For simplicity reasons in the setup of the field evaluation, the trajectory of the particle will be assumed to be strictly circular in dipole magnet models. Figure 6 shows from various angles how the actual trajectory of an electron in the magnet's field and a circular approximation diverge in the end, outside the magnet, when the fringe fields become too low to maintain the circular shape of the particle trajectory. The evaluations those two trajectories give for field integral should be close, for they only differ in regions that will not affect much the outcome of the field integration for the field strength there is lower. Data regarding the definition of the circular trajectory is given in table 1.

Trajectory data		
magnet modeled	AB'H'	
radius of curvature	1592.5	cm
sagitta	0.785	cm
Xcenter	1592.1075	cm
starting angle	-90	deg
end angle	-87.3	deg
bending angle	3.6	deg
total 1/2 angle incl. outer 25cm	2.7	deg

Table 1: Data defining the circular trajectory of reference. The position 'Xcenter' will vary to evaluate the variation of the integral of the vertical component of the field, thus giving us the normal quadrupole component according to equation (2). The sagitta and bending angle are design parameters.

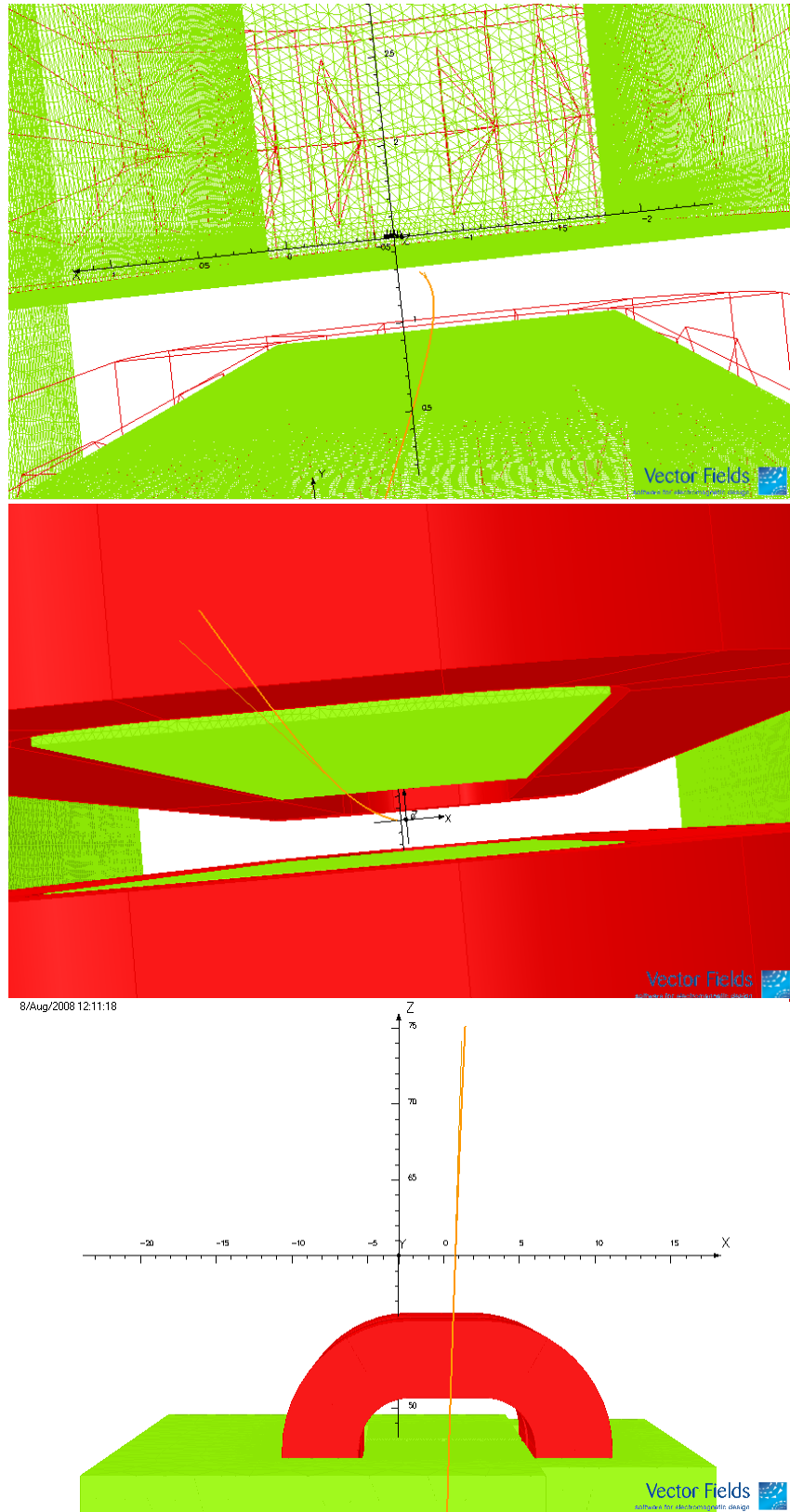


Fig. 6: Comparison between a circular trajectory (bold) and a trajectory with same starting point but calculated by the particle tracking function of the Opera post processor. The divergence is only obvious in the fringe fields outside the magnet. Since it is simpler and faster to introduce in the calculations, the circular path will be used so that this study reaches its conclusions faster, although a confirmation could be necessary in a second time using trajectories as realistic as possible.

## II.2 - Results

### II.2.1 - Field evaluation by nodal interpolation

The first calculation made consisted in realizing 10(+1) integrals, over trajectories whose relative initial 'x' position would vary between -1mm and +1mm with respect to the reference trajectory (Table 2). Each trajectory consists of 1000 points.

Relative x (cm)	x center (cm)	By integral half trajectory (G.cm)	full trajectory (G.cm)
-0.1	1592.0075	-7.002429173868490E+05	-1.400485834773700E+06
-0.08	1592.0275	-7.002443908297820E+05	-1.400488781659560E+06
-0.06	1592.0475	-7.002452040264560E+05	-1.400490408052910E+06
-0.04	1592.0675	-7.002445804347790E+05	-1.400489160869560E+06
-0.02	1592.0875	-7.002417373441280E+05	-1.400483474688260E+06
0	1592.1075	-7.002392229385580E+05	-1.400478445877120E+06
0.02	1592.1275	-7.002382521527560E+05	-1.400476504305510E+06
0.04	1592.1475	-7.002364974164070E+05	-1.400472994832810E+06
0.06	1592.1675	-7.002345164391390E+05	-1.400469032878280E+06
0.08	1592.1875	-7.002321758251870E+05	-1.400464351650370E+06
0.1	1592.2075	-7.002283350778150E+05	-1.400456670155630E+06

Table 2: Summary of the values of By integrals used to compute the first derivatives, plotted in figure 7.

Then  $\frac{\partial}{\partial x} \int B_y dl$  was calculated:

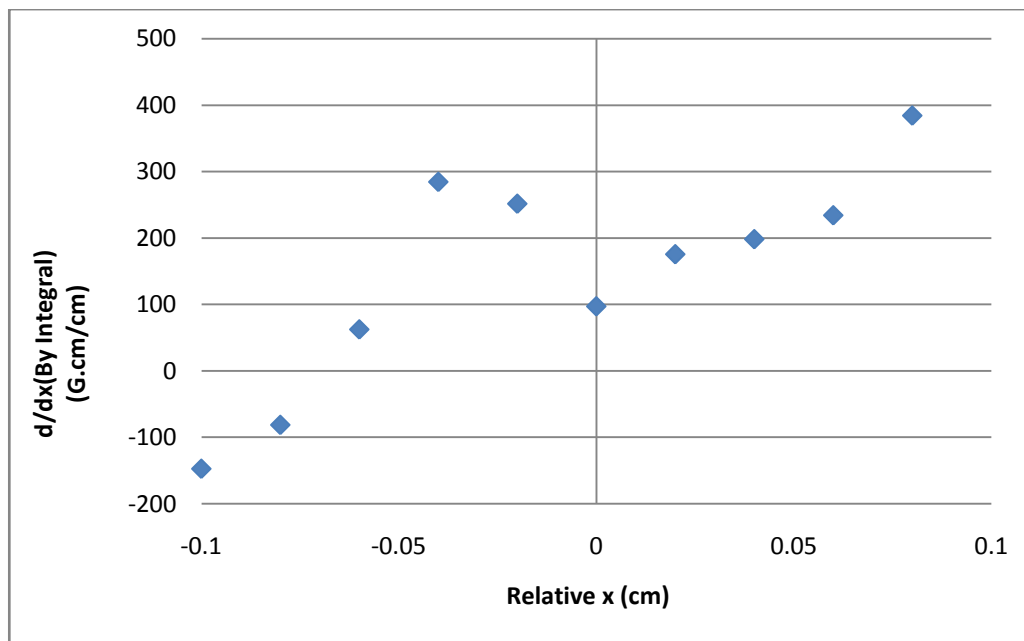


Fig. 7: First plot of the values of the derivatives calculated from the integrated By values of Table 2.



Since the graph on Figure 7 is too erratic to be used it was decided to try and use a finer step. The same evaluation was then run for 100 and 1000 trajectories (Fig. 8).

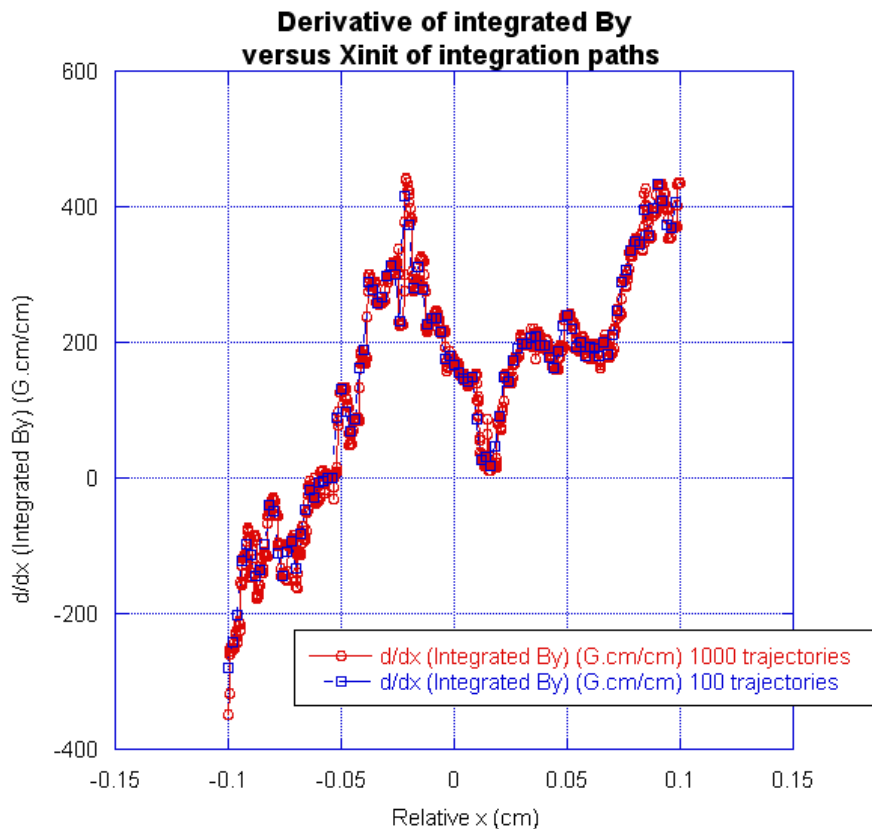


Fig. 8: Same as figure 7, with a step 10 times (blue) and 100 times (red) finer between the positions of the trajectories used for the integrals. Still quite shapeless.

This plot is still very erratic (its variations reach 2 orders of magnitude) and doesn't obviously allow to compute a normal quadrupole from the variation of Integrated By.

After a fruitless attempt to average the values of the integrals over several trajectories in order to smoothen the derivative curve (Figure 9 and 10), it was decided that the nodal interpolation method of evaluating the fields was far too dependent on mesh density and that the alternate method using integrals over the surfaces of the sources should be used instead, in spite of its tremendous slowness (~30 min per trajectory integral).

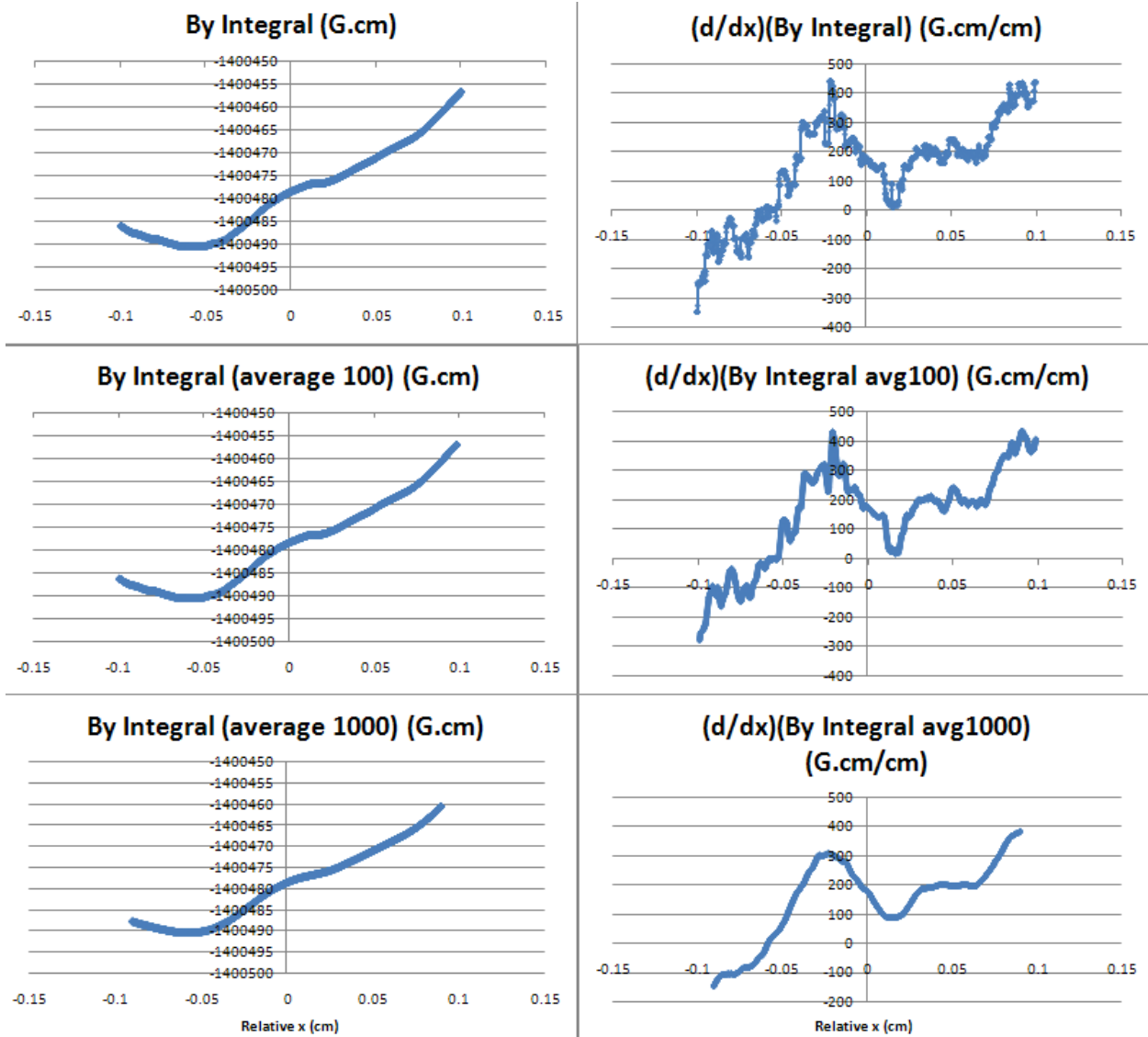


Fig. 9 : By integrals and their derivatives evaluated by nodal interpolation. This set has 10,000 points. The first 2 graphs are not averaged, the 4 latter use an average on 100 and on 1000 points.

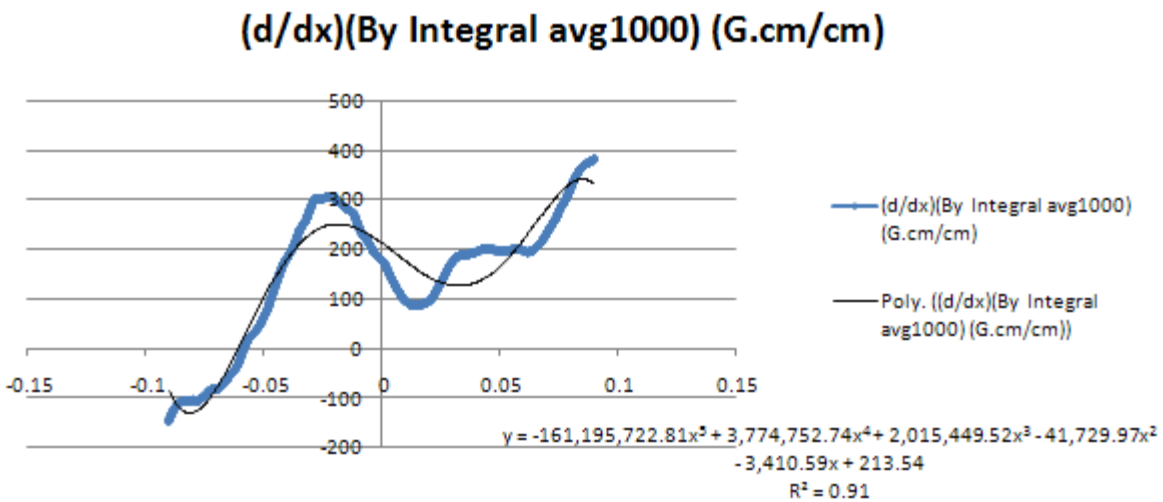


Fig. 10: Attempt to determine a polynomial fit for the most smoothed curve.

## II.2.2 - Field evaluation by surface integrals

As the field evaluation method using interpolation between nodes turned out to be unable to allow a normal quadrupole calculation, the same process was followed again using integrals over the surfaces of the sources. Since these evaluations take much longer, the number of trajectories as well as the number of evaluation points on the trajectories was reduced.

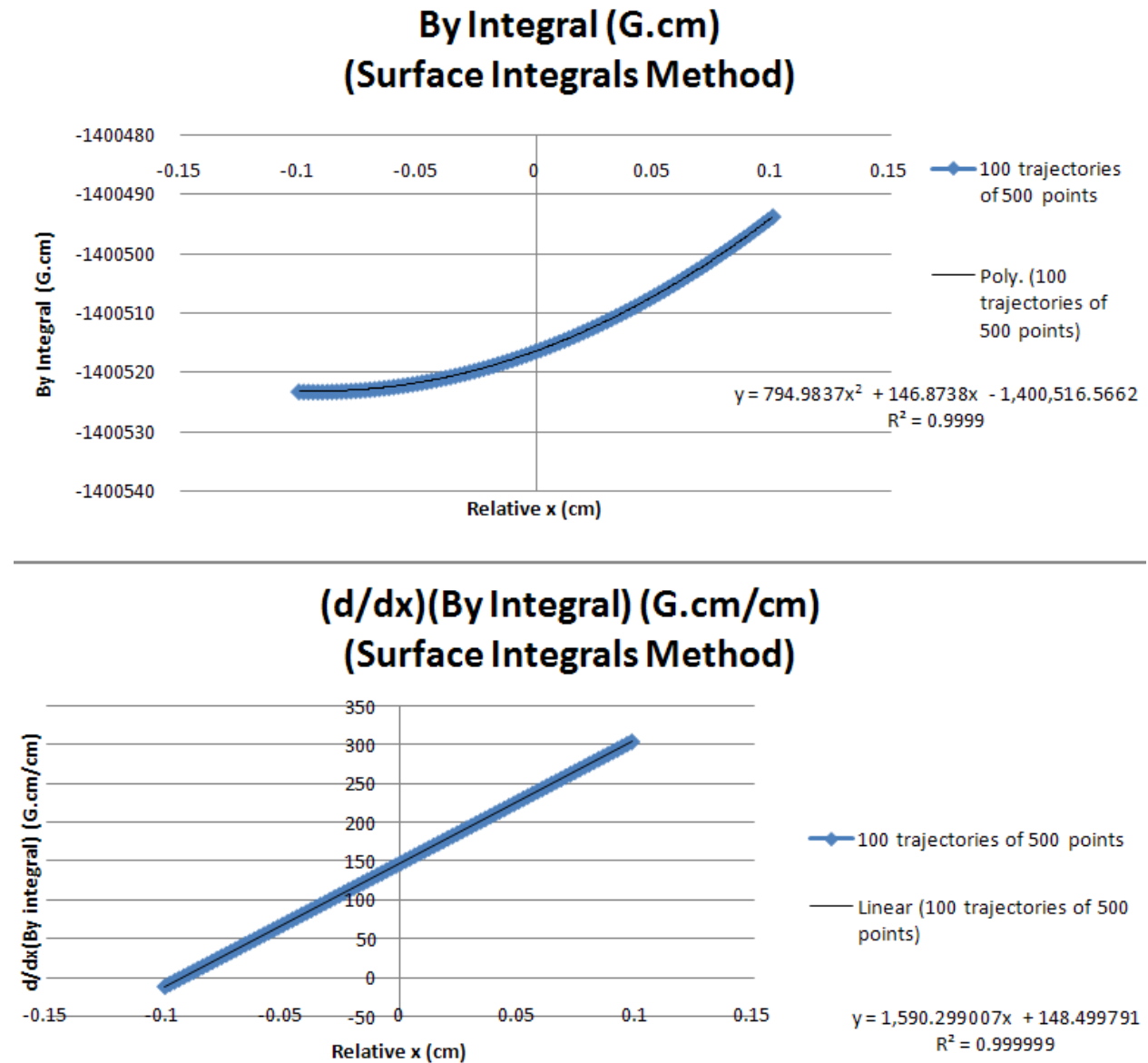
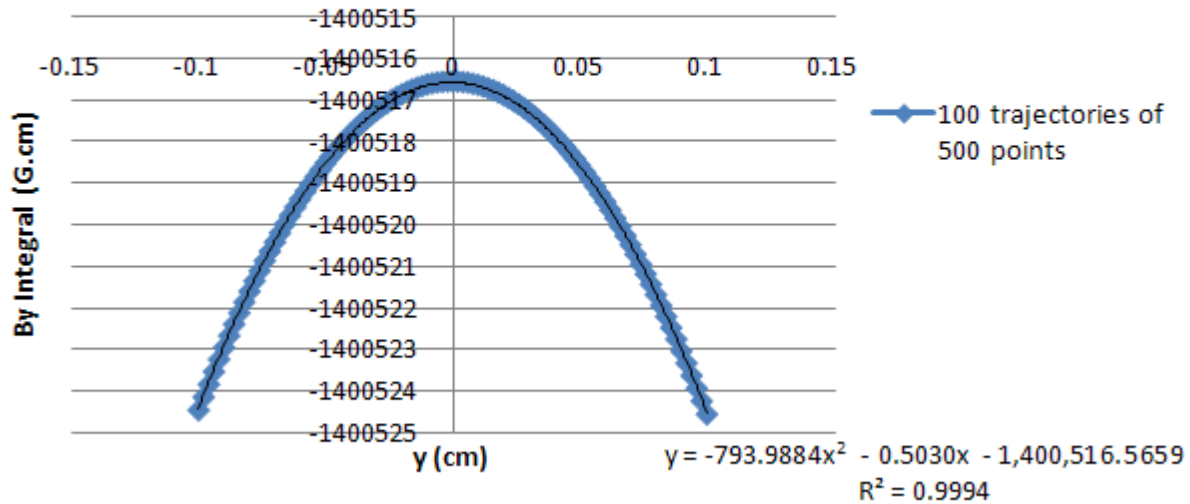


Fig. 11: By integral and its derivative with respect to x evaluated using the surface integrals method. The calculation was made using 100 trajectories of 500 points each.

## By Integral (G.cm) (Surface Integrals Method)



## d/dy(By integral) (G.cm/cm) (Surface Integrals Method)

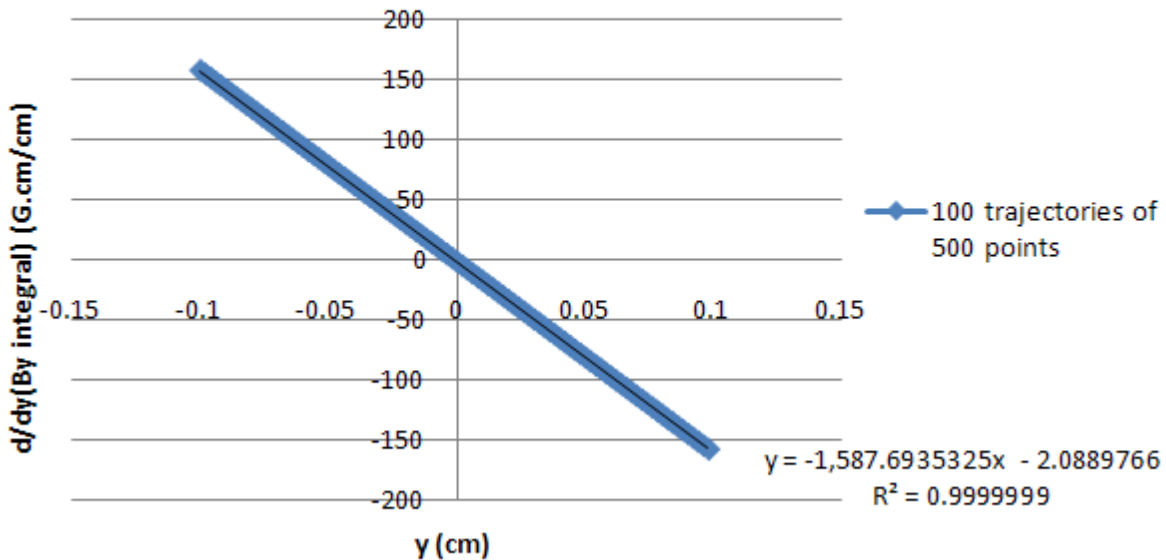


Fig. 12: By integral and its derivative with respect to y evaluated using the surface integrals method. The calculation was made using 100 trajectories of 500 points each.

This second method of evaluation is obviously less affected by mesh coarseness for numerical noise is imperceptible ( $R^2 > .99$  on every plot). Those results will therefore be considered as more reliable than those from the previous evaluation method.

### Interpretation

The field gradient presents a linear dependency on  $x$  and on  $y$ , which is a characteristic of a sextupole component. The constant term in the gradient represents the quadrupole term. Since the fits are applied to values that represent an integration over a 98cm-long dipole, we deduce that the components that are observed are:

Normal terms of field expansion along $x$	
Dipole	-14,587 G
Quadrupole	1.5297 G/cm
Sextupole	8.2800 G/cm <sup>2</sup>
Normal terms of field expansion along $y$	
Dipole	-14,587 G
Quadrupole	-0.0052 G/cm
Sextupole	-8.2697 G/cm <sup>2</sup>

Table 3: Summary of the first normal multipole terms of the field expansions along  $x$  and  $y$  respectively.

### III - Reconciliation

#### III.1 - Presentation

The idea of reconciliation between the two previously presented methods comes from the assumption that the circle method (Chap. I) gives inaccurate results because it does not take geometrical effects (path curvature...) into account (Fig. 3).

According to the equations of motion in the approximation of linear beam dynamics [2],

$$x'' + \left(\frac{1}{\rho_0^2} + k_0\right)x = 0 \quad (4)$$

the field evaluation method using small circles allows to compute  $k_0$  as the local field gradient but ignores the effect of the term  $\frac{1}{\rho_0^2}$  which represents the geometrical effect, the constant curvature that is responsible for weak focusing in the bending plane in sector magnets for example.

The idea therefore emerged that it may be possible to reconcile those two evaluation methods by computing independently the effect of local gradient and the geometrical effect and by comparing their combined influence with the result of the second evaluation method (Chap. II), using focal lengths:

$$\frac{1}{f_{\text{trajectory integrals}}} \stackrel{?}{=} \frac{1}{f_{\text{geom}}} + \frac{1}{f_{\text{stepcircles}}} \quad (5)$$

If (5) was verified, that would confirm that the only difference between the evaluation methods developed in sections I and II (using local circles and trajectory integrals respectively) is the geometrical effect mentioned earlier.

#### III.2 - Results

It was decided that formula (5) would be tested in the case of our rectangular 'ABH' magnet. The basic data concerning this magnet are given in Table 4:

Rectangular magnet data				
Parameter	symbol	value	unit	comments
Radius of trajectory curvature inside magnet	$\rho_0$	1592.5	cm	
Deviation Angle	$\theta$	3.6	deg	
	"	0.062832	rad	
Half Gap Height	h	1.295	cm	
Straight magnet length	L	96.012	cm	
Central B field	B	14178.4	G	
Curved length of reference trajectory	l	100.0597	cm	$\rho_0 \cdot \theta$

Table 4: Characteristics of the magnet that will be used for upcoming calculations

Tables 5 to 7 summarize the values obtained for the focal lengths needed in equation (5).

Geometrical term		
focal length	25345.4247	cm

Data from local circles method	value	unit
Full length integral of quadrupole	-733.01	G
Equivalent gradient	-7.33	G/cm
focal length	-30803.24	cm

Data from curved integrals method		
Normal terms of field expansion along x		
Dipole	-13,997	G
Quadrupole	1.4679	G/cm
focal length	153731.312	cm

Tables 5, 6, 7: Results obtained in the case of the 'ABH' magnet for each of the 3 focal lengths (highlighted) appearing in formula (5).

The geometrical term was obtained using [2]:

$$\frac{1}{f_{geom}} = \frac{l}{\rho_0^2} \quad (6)$$

The field gradients ( $G_{x,y}$ ) were expressed as focal lengths using:

$$f_{x,y} = \frac{B \cdot \rho_0}{G_{x,y} \cdot l} \quad (7)$$

The thin lens approximation assumed in equations (5), (6) and (7) turns out to be reasonable as the focal lengths that were obtained using it (tables 5, 6 and 7) are 2 to 3 orders of magnitude bigger than the length of the magnet (table 4).

Table 8 gives the actual inverses of the focal lengths and compares the RHS and LHS (underlined) of equation (5).

comparison chart		
invert focal lengths	values	units
from curved integrals	<u>6.50E-06</u>	<u>cm<sup>-1</sup></u>
from geometrical term	3.95E-05	cm <sup>-1</sup>
from stepped circles	-3.25E-05	cm <sup>-1</sup>
sum(stepped circles, geometrical term)	<u>6.99E-06</u>	<u>cm<sup>-1</sup></u>
concordance		
taking B = B(0,0,0)	7.5	%
taking B = dipole term evaluated with trajectory integrals method	0.3	%

Table 8: Summary of the terms of equation (5). LHS and RHS are underlined for easier reading. Their concordance in % is given in the lower part of the table. They match to 7.5% using the data given in table 4. Note that if instead of B(0,0,0), the value used for the norm of the field B is the dipole term coming from trajectory integrals (table 7), sides of equation (5) match to 0.3%.

B(0,0,0) was taken in the first place as a quick evaluation of the dipole field of the magnet. Since it's just representative of one point, through which the beam doesn't even pass, it's not very accurate though even if the order of magnitude is respected. On the other hand, the dipole term computed out of the evaluation of the integrated field along the particles trajectories is much more representative of what the beam actually witnesses as it goes through the magnet.

The reconciliation is therefore considered a success.



## IV - Conclusions and suggestions

### IV.1 - Conclusions

1. A new method for evaluating normal quadrupole in Opera/TOSCA 3D models was accurately developed, that allowed to upgrade the method used hitherto by broadening our understanding of it.
2. In spite of its being very time consuming, the new method is more direct and simpler than the older one and could turn out to be more interesting when it comes to normal multipoles if it was optimized to take advantage of its accuracy to reduce its time consumption.

### IV.2 - Suggestions

The following list is a set of suggestions and comments for anyone interested in continuing this study:

- As mentioned in the introduction of section II, the trajectories used in this study are mere circles. One way of refining the results of the evaluations is to use the realistic trajectory of an electron instead, that could be obtained by using the Opera post processor particle tracking possibilities.

- A possible way of taking advantage of the speed of the first method while keeping in mind the idea of the second might be to simply orient all the local circles so that they are normal to  $\vec{z}$  at all times. The advantage is that the field gradient is therefore evaluated in a classical Euclidian reference frame instead of the curved path frame, although the analogy with the measuring process that is used in reality is lost and only the accuracy of the integrated result would be interesting, abandoning local relevance (the circles would not be normal to the trajectory anymore). One should also be aware (a) that this whole idea relies on a small beta phase advance assumption (i.e. distance between parallel incident particles is conserved in the system) and (b) that the step between the circles should be a constant with respect to the beam curved path length and not with respect to  $\vec{z}$  so that places where beam trajectory has strongest angle with respect to  $\vec{z}$  direction are not underrepresented in the integration.

- The 1-cm radius of the circles used in the first method was constrained by local mesh density. One should be aware though, that it was established [3] that field evaluation using surface integrals is not influenced by local mesh density, which might give a degree of freedom regarding the radii of the circles. Another argument favoring a reduction of their radii is that the noise in the integration method comes from " higher order solution errors decreasing rapidly with distance from the sources " [3], which might be efficiently reduced if the circles get less close to the poles.

## *Acknowledgements*

I want to deeply thank my supervisor Jay Benesch and our colleagues Michael Tiefenback and Yves Roblin for their patience and availability throughout countless enlightening discussions that made this study possible.

## *References*

- [1]: Opera Version 12.009 Professional Edition x64, Vector Fields Ltd, 24 Bankside, Kidlington, Oxford, OX5 1JE, UK, support@vectorfields.co.uk, <http://www.vectorfields.com>
- [2]: H. Wiedemann: *Particle Accelerator Physics I Basic Principles and Linear Beam Dynamics*, Second Edition, ed. by Springer Study, Chap. 5 (2003)
- [3]: N. Ruiz: *Higher order field multipoles dependence on machining defects*, JLAB-TN-08-062, 2008